

Active Geometric Wavelets

Itai Gershtansky¹ and Shai Dekel²

Abstract: We present an algorithm for highly geometric sparse representation. The algorithm combines the adaptive Geometric Wavelets method with the Active Contour segmentation to overcome limitations of both algorithms. It generalizes the Geometric Wavelets by allowing to adaptively construct wavelets supported on curved domains. It also improves upon the Active Contour method that can only be used to segment a limited number of objects. We show applications of this new method in medical image segmentation.

¹ Tel-Aviv University

² GE Healthcare

1 Introduction

The *Active Contour (Level-Set)* method is a well known approach for image segmentation [2, 11,13]. It is general enough to allow definition of different cost functions, in order to identify different types of objects in the image, but at the same time, it is also relatively simple to implement. It is also popular because it provides actual segmentation represented by continuous curves, whereas other ‘edge detection’ methods only compute the probability that a pixel is an ‘edge’ pixel or that a pixel belongs to an ‘object’.

The main problem of the existing Active Contour methods is that it is limited to segmenting out a small number of objects (see an attempt to fix this in [3]). Our approach tries to overcome this issue, by applying local segmentations locally and recursively. The result is a multiresolution tree structure of disjoint sub-regions over which one may construct a highly geometric wavelet representation of the image. This approach generalizes the previous construction of *Geometric Wavelets (GW)* [5] where the recursive subdivision was applied using only straight lines, producing convex polygonal regions. We now recall the GW algorithm:

Given a function $f : [0,1]^2 \rightarrow [0,1]$ over the unit cube, it is subdivided using a line segment to two sub-regions Ω_1, Ω_2 such that

$$\|f - Q_{\Omega}\|_{L_2(\Omega)}^2 + \|f - Q_{\Omega'}\|_{L_2(\Omega')}^2, \quad (1.1)$$

is minimized, where $Q_{\Omega}, Q_{\Omega'}$ are polynomials of some fixed low order. Note that for each candidate bisection, the optimal polynomials are given by the least squares method. This process continues recursively, until a stopping criterion is met, typically when (1.1) is below a given threshold. Observe that the sub-regions are always convex polyhedral domains, which is a crucial property when approximating with piecewise polynomials (see discussion in Section 2).

The result of this algorithm is a *Binary Space Partition (BSP)* tree, \mathcal{P} composed of pairs $\{(\Omega, Q_{\Omega})\}$: the sub-regions and the approximating polynomials constructed over them. The root of the tree is $([0,1]^2, Q_{[0,1]^2})$, where $Q_{[0,1]^2}$ is the approximation of the function over the unit cube. This tree can be used to define an adaptive Geometric Wavelet decomposition of the function in the following way. If (Ω, Q_{Ω}) is the father of $(\Omega', Q_{\Omega'})$, define

$$\psi_{\Omega'} := \psi_{\Omega'}(f) := 1_{\Omega'}(Q_{\Omega'} - Q_{\Omega}), \quad (1.2)$$

as the geometric wavelet associated with the sub-region Ω' and the function f . The low resolution component, associated with the root of the BSP tree is

$$\psi_{[0,1]^2} := Q_{[0,1]^2}. \quad (1.3)$$

The wavelets (1.2) are in fact a ‘local difference’ components that belong to the detail space between two levels in the BSP tree, a ‘low resolution’ level associated with Q_Ω and a ‘higher resolution’ level associated with $Q_{\Omega'}$. The GW method follows the classical procedure of n -term wavelet approximation ([4], [6]): The importance of the wavelet is measured by its L_2 norm, and so we reorder:

$$\|\psi_{\Omega_{k_1}}\|_2 \geq \|\psi_{\Omega_{k_2}}\|_2 \geq \|\psi_{\Omega_{k_3}}\|_2 \geq \dots \quad (1.4)$$

Given an integer $n \in \mathbb{N}$, we have the n -term approximation

$$\psi_{[0,1]^2} + \sum_{i=1}^n \psi_{\Omega_{k_i}}. \quad (1.5)$$

It can be shown that under mild condition on the BSP tree and the function f ,

$$f = \sum_{\Omega \in \mathcal{P}} \psi_\Omega(f).$$

Since edge singularities in images are in general not line segments, the above method will require bisections at several levels of the BSP tree to approximate them. To this end, we enhance the method of [5], by using more advanced segmentation algorithms at each recursive subdivision step. Instead of minimizing (1.1), we minimize a Mumford-Shah type functionals such as [2]

$$\|f - Q_{in(\gamma)}\|_{L_2(in(\gamma))}^2 + \|f - Q_{out(\gamma)}\|_{L_2(out(\gamma))}^2 + \mu \cdot \text{length}(\gamma), \quad (1.6)$$

where γ is a closed curve and $in(\gamma)$ and $out(\gamma)$ are its inside and outside domains, respectively. The first two terms are the penalties for approximation over the two sub-regions and the third term is the penalty for curve length. Again, for each fixed curve, the approximation polynomials are uniquely determined by the least squares method. There are numerous variants to (1.6) and numerical algorithms to compute them. These algorithms are all iterative and most of them are highly sensitive to the input initial curve. In our algorithm we also use a more localized level-set variation [10] that works well if the initialization curve is ‘close’ to the solution curve. For some given $\varepsilon > 0$, let $\delta(\phi)$ be an approximation to the Dirac of ϕ

$$\delta(\phi) := \begin{cases} \frac{1}{2\varepsilon} \left(1 + \cos\left(\frac{\pi\phi(x)}{\varepsilon}\right) \right), & 0 \leq \phi(x) \leq \varepsilon, \\ 0, & \text{otherwise,} \end{cases}$$

and denote for some pre-determined radius r

$$\beta_r(x, y) := \begin{cases} 1, & |x - y| \leq r, \\ 0, & \text{otherwise.} \end{cases}$$

Then, a ‘local’ energy functional is given by

$$E(\phi) := \int_{\Omega} \delta\phi(x) \int_{\Omega} \beta_r(x, y) F(I(y), \phi(y)) dy dx + \mu \int_{\Omega} \delta\phi(x) |\nabla\phi(x)| dx, \quad (1.7)$$

where F is an ‘internal’ energy term (see the details of [10]).

Our *Active Geometric Wavelet (AGW)* algorithm for sparse representation is thus composed of 3 steps:

- A. **Initialization** - In the first step we try to find connected groups of pixels with similar values. The outer boundaries of these connected groups are used as initial guesses for the segmentation algorithm in the second step.
- B. **Construction of the geometric BSP tree** - Since the contours computed in step A are expected to be close to objects in the image, the segmentation is computed with the localized functional (1.7). In case this segmentation gives an error larger than a given threshold, we switch to the functional (1.6) and continue the subdivision process. The recursive application of these active contour segmentations creates a geometric BSP tree structure over the image.
- C. **Creation of the n -term approximation** - An approximating wavelet sum is created according to (1.4) and (1.5).

The paper is organized as follows. In section 2 we provide the theoretical foundation for the AGW method. In Section 3 we describe the algorithm in detail and in section 4 show numerical examples for Computed Tomography (CT) images.

2 Theoretical background

2.1 A Jackson estimate for piecewise polynomial approximation using non-convex domains

Let $\Pi_{r-1}(\mathbb{R}^d)$ denote the multivariate polynomials of total degree $r-1$ (order r) in d variables. Our objective is to approximate a given function by low order polynomials over a possibly non-convex sub-

domains. For polynomial approximation over a single convex domain there is a complete characterization of the degree of approximation by smoothness measures such as the modulus of smoothness and K -functional, where the constants are universal over all convex domains (see [5] and references therein). However, the situation is essentially different when approximating over non-convex domains (see examples in [9]).

In the following we define the notion of an α -class that quantifies how ‘close’ a given domain is to being convex. We then give a Jackson estimate for an n -term approximation using piecewise polynomials over sub-domains all in the same α -class.

Definition 2.1 Let $\alpha \geq 1$. We say that a bounded domain $\Omega \subset \mathbb{R}^d$ belongs to the α -class if there exist an ellipsoid θ such that $\theta \subseteq \Omega \subseteq \theta_\alpha$, where θ_α is the α -blowup of θ

$$\theta_\alpha := \{v_\theta + \alpha(x - v_\theta) : x \in \theta\}, \quad v_\theta \text{ center of } \theta.$$

John’s Lemma [7] proves that all bounded convex domains in \mathbb{R}^d are in the d -class. In some sense, the notion of the α -class improves upon the ‘Chunkiness Parameter’ [1] which is frequently used in the Finite Element Method literature to evaluate the shape of a given domain for the purpose of local polynomial approximation. The ‘Chunkiness Parameter’ relates to the ratio between a minimal enclosing ball and maximal contained ball, so in this sense using ellipsoids is better for long and thin, but possibly non-convex domains. The following lemma is a generalization of Lemma 2.4b from [5], where it was proved for convex domains.

Lemma 2.2 For any Ω that belongs to α -class, $P \in \Pi_{r-1}(\mathbb{R}^d)$ and $0 < p, q \leq \infty$ we have

$$\|P\|_{L_q(\Omega)} \sim |\Omega|^{1/q-1/p} \|P\|_{L_p(\Omega)},$$

with constants of equivalency depending on d, r, p, q and α .

Proof By the equivalency of finite dimensional Banach spaces, we have that $\|P\|_{L_p(B(0,1))} \sim \|P\|_{L_q(B(0,\alpha))}$, for any polynomial $P \in \Pi_{r-1}(\mathbb{R}^d)$, where $B(0,l) = \{x \in \mathbb{R}^n : |x| \leq l\}$, with constants of equivalency depending only on p, q, d, r and α . Since Ω is in the α -class, there exists an ellipsoid $\theta \subseteq \Omega$ and an affine transformation A_θ , $A_\theta x = M_\theta x + v_\theta$, satisfying $A_\theta(B(0,1)) = \theta$, for which

$$B(0,1) \subseteq A_\theta^{-1}(\Omega) \subseteq B(0,\alpha).$$

Therefore,

$$\begin{aligned}
\|P\|_{L_q(\Omega)} &= |\det M_\theta|^{1/q} \|P(A_\theta \cdot)\|_{L_q(A_\theta^{-1}(\Omega))} \leq |\det M_\theta|^{1/q} \|P(A_\theta \cdot)\|_{L_q(B(0,\alpha))} \\
&\leq c |\det M_\theta|^{1/q} \|P(A_\theta \cdot)\|_{L_p(B(0,1))} \leq c |\det M_\theta|^{1/q} \|P(A_\theta \cdot)\|_{L_p(A_\theta^{-1}(\Omega))} \\
&\leq c |\det M_\theta|^{1/q-1/p} \|P\|_{L_p(\Omega)}.
\end{aligned}$$

□

We can now apply the machinery introduced in [8] to obtain a Jackson estimate. The following theorems are in fact Theorem 3.3 and Theorem 3.4 from [8], formulated in a general enough manner that allows us to apply them for the case of piecewise polynomial approximation over general subdomains.

Theorem 2.3 Suppose $\{\Phi_m\}$ is a sequence of functions in $L_p(\mathbb{R}^d)$, $0 < p < \infty$, which satisfies the following additional properties when $1 < p < \infty$

- (i) $\Phi_m \in L_\infty(\mathbb{R}^d)$, $\text{supp } \Phi_m \subset E_m$ with $0 < |E_m| < \infty$, and $\|\Phi_m\|_\infty \leq c_1 |E_m|^{-1/p} \|\Phi_m\|_p$.
- (ii) If $x \in E_m$, then

$$\sum_{x \in E_j, |E_j| \geq |E_m|} \left(\frac{|E_m|}{|E_j|} \right)^{1/p} \leq c_1,$$

where the summation is over all indices j for which E_j satisfies the indicated conditions.

Denote (formally) $f := \sum_m \Phi_m$ and assume that for some $0 < \tau < p$

$$N(f) := \left(\sum_m \|\Phi_m\|_p^\tau \right)^{1/\tau} < \infty. \tag{2.1}$$

Then $\sum_m |\Phi_m(\cdot)| < \infty$ a.e. on \mathbb{R}^d , and hence, f is well defined. Furthermore, if $1 \leq p < \infty$, condition (2.1) can be replaced by the weaker condition

$$N(f) := \left\| \left\{ \|\Phi_m\|_p \right\} \right\|_{wl_\tau} < \infty, \tag{2.2}$$

where $\left\| \{x_m\} \right\|_{wl_\tau}$ denotes the weak l_τ -norm of the sequence $\{x_m\}$:

$$\left\| \{x_m\} \right\|_{wl_\tau} := \inf \left\{ M : \#\{m : |x_m| > Mn^{-1/\tau}\} < n \text{ for } n = 1, 2, \dots \right\}.$$

Theorem 2.4 Under the hypothesis of Theorem 2.3, suppose $\{\Phi_m^*\}_{j=1}^\infty$ is a rearrangement of the sequence $\{\Phi_m\}$

such that $\|\Phi_1^*\|_p \geq \|\Phi_2^*\|_p \geq \dots$. Denote $S_n := \sum_{j=1}^n \Phi_j^*$. Then

$$\|f - S_n\|_p \leq cn^{-\beta} N(f) \quad \text{with } \beta = 1/\tau - 1/p, \quad (2.3)$$

where $c = 1$ if $0 < p \leq 1$ and $c = c(\beta, p, c_1)$ if $1 < p < \infty$. Furthermore, the estimate remains valid if condition (2.1) can be replaced by (2.2) when $1 \leq p < \infty$.

We first observe that if the AGW method uses piecewise constants, then we actually have equality in condition (i) of Theorem 2.3 for any type of domain. For higher order polynomials, we need to assume that the domains are in the α -class for some fixed α and then we obtain condition (i) by application of Lemma 2.2. Also, if each step of the recursive subdivision bisects a domain into sub-domains of relatively ‘substantial’ area, then also condition (ii) of Theorem 2.3 is satisfied. The quantity $N(f)$ should be considered as a ‘geometric sparsity gauge’ for the function f . It will be typically very small for cartoon-type images, if the domains of the Active Geometric Wavelets are aligned with the curve singularities. In these settings, Theorem 2.4 says that a ‘greedy’ n -term approximation based on AGW performs well.

2.2 Adaptive local selection of the weight μ

One of the key elements of the AGW algorithm is a correct choice of the parameter μ in (1.6). A possible strategy is the following: As an initial guess, choose a large value of the parameter, one that gives an empty segmentation, that is, a segmentation where all the pixels are considered to be ‘outside’. Then, gradually, diminish the value of μ , until some segmentation is achieved. As a motivation for this strategy we consider minimizing the Chan-Vese functional (1.6) over the simple indicator function of a circle. More formally, suppose we have an function I defined on the cube $[0,1]^2$. We would like to minimize

$$M(\mu) = M(\gamma, c_1, c_2, \mu) = \int_{in(\gamma)} (I - c_1)^2 + \int_{out(\gamma)} (I - c_2)^2 + \mu \cdot \text{length}(\gamma), \quad (2.4)$$

where $\gamma : [0,1] \rightarrow [0,1]^2$ is any closed curve. $in(\gamma)$ is the region (or union of regions) that is (are) inside γ (including the boundary of γ) and $out(\gamma)$ is the complement of $in(\gamma)$ in $[0,1]^2$. More specifically, we wish to investigate the dependence of the solution on μ .

Theorem 2.5 Let $I : [0,1]^2 \rightarrow [0,1]$ the characteristic function of a circle $C = \{x \in [0,1]^2 : |x - x_0| \leq a\} \subset [0,1]^2$

where $0 < a < \sqrt{0.5/\pi}$. Then with $\mu_0 = 0.5a(1 - \pi a^2)$ we have

$$\min M(\mu) = \begin{cases} \pi a^2(1 - \pi a^2), & \mu_0 \leq \mu, \\ 2\mu\pi a, & 0 \leq \mu \leq \mu_0, \end{cases} \quad \arg \min M(\mu) = \begin{cases} \gamma_\emptyset, & \mu_0 \leq \mu, \\ \gamma_C, & 0 \leq \mu \leq \mu_0, \end{cases} \quad (2.5)$$

where γ_\emptyset is the empty curve, for which $out(\gamma_\emptyset) = I$, $in(\gamma_\emptyset) = \emptyset$ and $\gamma_C = \partial C$.

Remark: We restrict ourselves to the case where the radius of the circle is sufficiently small, i.e.

$0 < a < \sqrt{0.5/\pi}$, so as to keep the image boundaries far from the object in question in order not to deal with some geometric issues that arise from such proximity. This is not a significant restriction and allows a simpler proof.

Proof of Theorem 2.5 For the proof we'll use the following definition:

$$\Gamma_{in}(\Omega) := \{\gamma : in(\gamma) \cap \Omega \subseteq \Omega\}, \quad \Gamma_{out}(\Omega) := \{\gamma : in(\gamma) \cap \Omega = \emptyset\},$$

for the set of all curves that are completely inside Ω , and the set of all curves that are completely outside it, respectively. Next, we calculate the penalty for approximation in a region where the function takes two values \setminus : an area of k_1 with value a_1 and an area of k_2 with value a_2 : the average is $(k_1 a_1 + k_2 a_2)/(k_1 + k_2)$ and the penalty is

$$k_1 \left(\frac{k_1 a_1 + k_2 a_2}{k_1 + k_2} - a_1 \right)^2 + k_2 \left(\frac{k_1 a_1 + k_2 a_2}{k_1 + k_2} - a_2 \right)^2 = \frac{k_1 k_2 (a_1 - a_2)^2}{(k_1 + k_2)}.$$

Let us first find $\arg \min_{\gamma \in \Gamma_{in}(C)} M(\mu)$. If $\gamma \in \Gamma_{in}$, then $length(\gamma) \leq 2\pi a$, otherwise $M(\gamma_C) < M(\gamma)$, because the

penalty for length for γ_C is smaller than that of γ and the sum of penalties for inner and outer approximation for γ cannot be smaller than that of γ_C , which is 0. Moreover, if the considered curve, γ , is not a circle, then according to the isoperimetric inequality, a circular curve with the same area will give a smaller value for M , because it will have a smaller length penalty. Thus, we may consider only the circular curves in Γ_{in} .

Denote the radius of γ as r and M becomes a function of r with $0 \leq r \leq a$. In this case, according to above calculation,

$$M(r) = \frac{(1 - \pi a^2)(\pi a^2 - \pi r^2)}{1 - \pi r^2} + 2\pi\mu r.$$

For a given μ we need to find $\inf_r M(r)$. We compute

$$\begin{aligned} M'(r) &= \frac{-2\pi r(1 - \pi a^2)(1 - \pi r^2) + 2\pi r(1 - \pi a^2)(\pi a^2 - \pi r^2)}{(1 - \pi r^2)^2} + 2\pi\mu \\ &= \frac{2\pi r(1 - \pi a^2)(\pi a^2 - 1)}{(1 - \pi r^2)^2} + 2\pi\mu = 2\pi \left(\mu - r \left(\frac{1 - \pi a^2}{1 - \pi r^2} \right)^2 \right). \end{aligned}$$

and

$$M''(r) = -2\pi \left(\frac{1 - \pi a^2}{1 - \pi r^2} \right)^2 \left(\frac{1 + 3\pi r^2}{1 - \pi r^2} \right) < 0.$$

The second derivative is always negative, which implies that the first derivative is strictly decreasing from $M'(0) = 2\pi\mu$ to $M'(a) = 2\pi(\mu - a)$.

If $\mu \geq a$, M' is always non-negative for $0 \leq r \leq a$, and so M non decreasing. Therefore, the minimum is obtained at $r = 0$. Since $\mu_0 < a \leq \mu$, this agrees with the first case in (2.5). If $\mu < a$, there's a parameter r for which $M'(r) = 0$ and M has a local maximum, since $M'' < 0$. Therefore, a global minimum is achieved at one of the end points $r = 0$, with $M(0) = \pi a^2(1 - \pi a^2)$ or $r = a$, with $M(a) = 2\mu\pi a$. If $M(0) < M(a)$, then $\pi a^2(1 - \pi a^2) < 2\mu\pi a$ which is exactly the condition $\mu_0 < \mu$, and this again agrees with the first case in (2.5). If $M(a) \leq M(0)$, then $\mu \leq \mu_0$ and this agrees with the second case in (2.5).

Next, we deal with the case where γ is not necessarily contained in the circle. We now describe M as a function of three variables: p, q and l , where

$$p := |\text{in}(\gamma) \cap C|, \quad q := |\text{in}(\gamma) \cap ([0, 1]^2 \setminus C)|, \quad l := \text{length}(\gamma).$$

The functional (2.4) now takes the form

$$M(p, q, l) = \frac{(1 - \pi a^2 - q)(\pi a^2 - p)}{1 - \pi a^2} + \frac{pq}{p + q} + \mu \cdot l,$$

where we observe that not all non-negative triplets (p, q, l) are geometrically feasible. Next we define a functional of two variables

$$Y(p, q) := \frac{(1 - \pi a^2 - q)(\pi a^2 - p)}{1 - \pi a^2} + \frac{pq}{p + q} + \mu \cdot \sqrt{4\pi(p + q)}.$$

Observe that by the isoperimetric inequality, for any curve γ , $\text{length}(\gamma) \geq \sqrt{4\pi(p + q)}$, with equality for circles and so $Y(p, q) \leq M(\gamma)$. Observe that if it is possible for some fixed pair p, q , to choose γ to be a circle, then this would imply $Y(p, q) = \min_{p, q, l \text{ feasible}} M(p, q, l)$. However, there are cases where this is not possible, such as where γ contains C and almost all of $I \setminus C$, with $p = \pi a^2$ and $q = 1 - \pi a^2 - \varepsilon$, for some small ε . In this case, γ cannot have the shape of a circle.

We now minimize Y over $A = [0, \pi a^2] \times [0, 1 - \pi a^2]$. We compute

$$\begin{aligned} \frac{\partial Y}{\partial p} &= \left(\frac{q}{p + q} \right)^2 - \left(\frac{1 - \pi a^2 - q}{1 - p - q} \right)^2 + 2\pi\mu(4\pi(p + q))^{-\frac{1}{2}}, \\ \frac{\partial Y}{\partial q} &= \left(\frac{p}{p + q} \right)^2 - \left(\frac{\pi a^2 - p}{1 - p - q} \right)^2 + 2\pi\mu(4\pi(p + q))^{-\frac{1}{2}}, \end{aligned}$$

and then

$$\begin{aligned} \frac{\partial^2 Y}{\partial p^2} &= -2q^2(p + q)^{-3} - 2(1 - \pi a^2 - q)(1 - p - q)^{-3} - 4\pi^2\mu(4\pi(p + q))^{-\frac{3}{2}}, \\ \frac{\partial^2 Y}{\partial q^2} &= -2p^2(p + q)^{-3} - 2(\pi a^2 - p)(1 - p - q)^{-3} - 4\pi^2\mu(4\pi(p + q))^{-\frac{3}{2}}. \end{aligned}$$

Observe that for $p > 0$ and $q > 0$, we have that $\partial^2 Y / \partial^2 p, \partial^2 Y / \partial^2 q < 0$. For a point to be a minimum it is necessary that $\partial^2 Y / \partial^2 p, \partial^2 Y / \partial^2 q > 0$, so there are no internal minimum points. On the lines $[0, \pi a^2] \times (1 - \pi a^2)$ and $\pi a^2 \times [0, 1 - \pi a^2]$, we have

$$\frac{\partial Y}{\partial p}(p, 1 - \pi a^2) > 0, \quad \frac{\partial Y}{\partial q}(\pi a^2, q) > 0,$$

so the minimum of Y is on the union of the two lines $A_{in} = [0, \pi a^2] \times 0$ and $A_{out} = 0 \times [0, 1 - \pi a^2]$.

Furthermore, for every point $z = (0, q) \in A_{out}$, the point $z' = (q, 0) \in A_{in}$ satisfies $Y(z') < Y(z)$, because

$$Y(z') = \pi a^2 - q < \pi a^2 - \frac{\pi a^2}{1 - \pi a^2} q = Y(z),$$

where we use the condition $\pi a^2 < 0.5$. The conclusion is that the minimum of Y is attained on A_{in} . On this line, M and Y have the same value, so the minimizer of Y is either $(p, q) = (0, 0)$ or $(p, q) = (\pi a^2, 0)$, as shown before.

Finally, the minimum of M over A is also attained at $(p, q) = (0, 0)$ or $(p, q) = (\pi a^2, 0)$; otherwise, the minimum for M is attained at some point $z \in A \setminus A_{in}$. Denote by z_0 the point for which Y attains its minimum on A_{in} (either $(p, q) = (0, 0)$ or $(p, q) = (\pi a^2, 0)$), then, $M(z_0) = Y(z_0) < Y(z) \leq M(z)$, which is a contradiction.

□

We conclude from the last result that for the simple case of a characteristic image of a circle, the approach of taking a large value of μ , i.e. $\mu > \mu_0(a)$, then reducing it until a non-empty segmentation is achieved ($\mu \leq \mu_0$), is indeed an approach that gives the required segmentation.

3 Overview of the AGW algorithm

The algorithm is composed of three stages: Initialization, construction of the BSP tree and building an approximation. In the first step we try to find contours that will serve as initial guesses for the segmentations. Since the level-set method is sensitive to the initialization, starting from a good initial guess is critical to the success of the algorithm. Therefore, we begin by searching for groups of pixels with relatively similar grey-level and sort these groups according to their set size. Sets with size smaller than a threshold are discarded. The result of applying this step on standard test images can be seen in Figures 1 and 2 below.

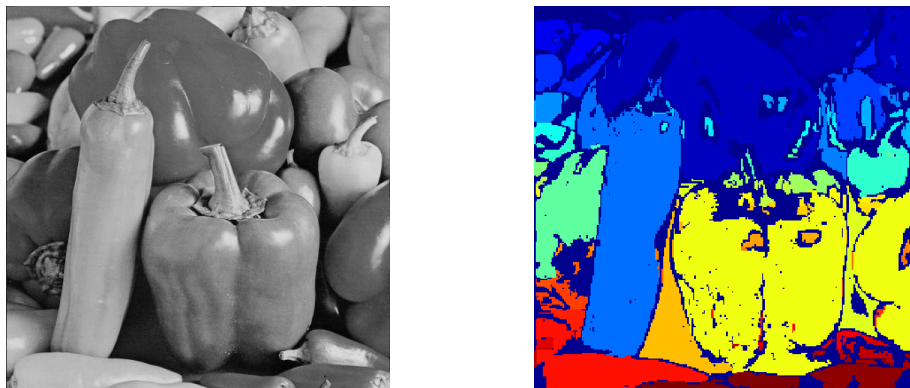


Figure 1: Initial pixel groups for the “Peppers” image

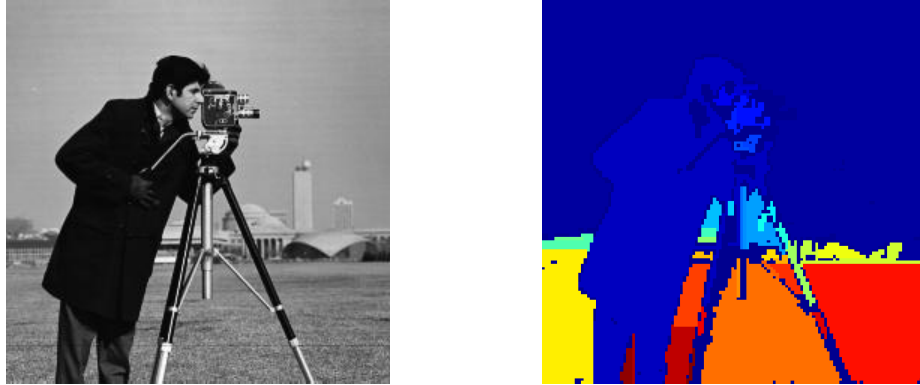


Figure 2: Initial pixel groups for the “Cameraman” image

In Figure 3 we see a Computed Tomography (CT) image and the pixel groups computed for this image. The goal in medical imaging is to segment correctly the various internal organs and perform certain measurements and analysis. We see that some key organs such as the kidneys and spine were not identified, since the imaging characteristics of these organs have higher variability. Therefore, to correctly identify initial pixel groups associated with these organs, we applied an anisotropic diffusion algorithm [12] to sharpen the edges and smooth the areas between them and then computed the pixel groups on this pre-processed image (Figure 4).

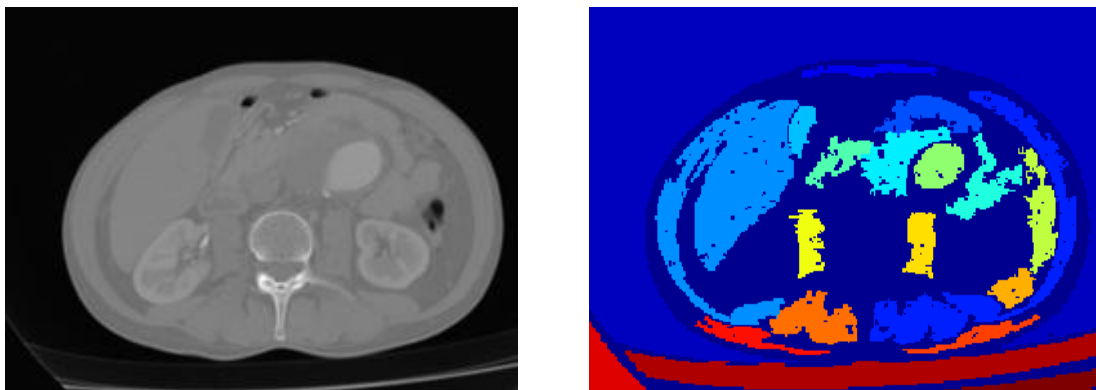


Figure 3: Initial pixel groups for a CT image

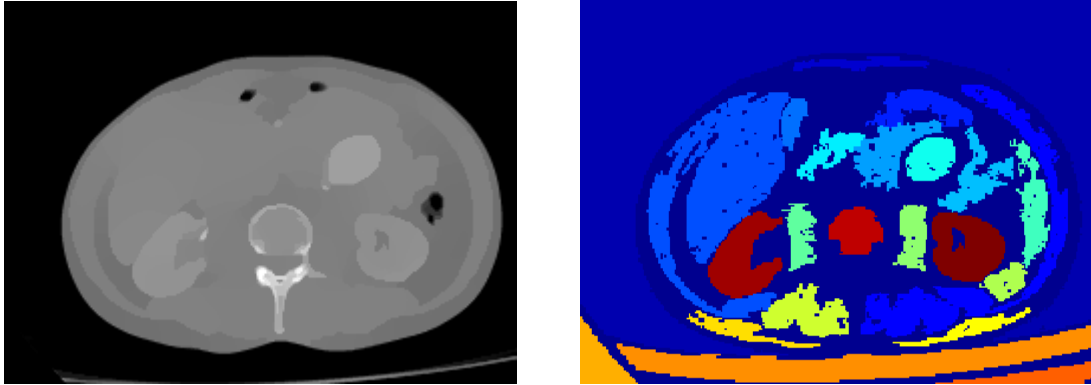


Figure 4: CT image after anisotropic diffusion and the pixel groups computed from it

In the second step, the algorithm builds the BSP tree. It minimizes the ‘local’ functional (1.7) with the outer contours of the pixel groups found in the first step, starting with the largest group and continuing in a diminishing order. Each of these iterations gives a bisection of a sub-region of the picture to an object and background and adds two new sibling nodes to the BSP tree at some level. If a pixel group is segmented, but the approximation error is above some required threshold, the algorithm continues to bisect it using a grid of circles as the initial guess and minimizing the ‘global’ functional (1.6).

In Figure 5 we see the initial guess for the first segmentation, obtained from the largest pixel group. In Figure 6 we see the segmentation computed from this initial guess. We see that the segmentation did not correctly segment the liver. This is exactly the weak point of a regular Active Contour algorithm that our method solves, because since the approximation error in this domain is found to be large, this domain will be further subdivided. In Figure 7 we see the grid of circles that serves as an initialization for the active contour segmentation of the first domain and in Figure 8 we see the correct segmentation appearing at the second level of the BSP tree.

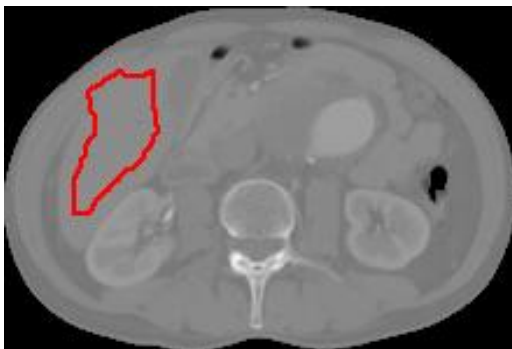


Figure 5: Initial guess for segmentation

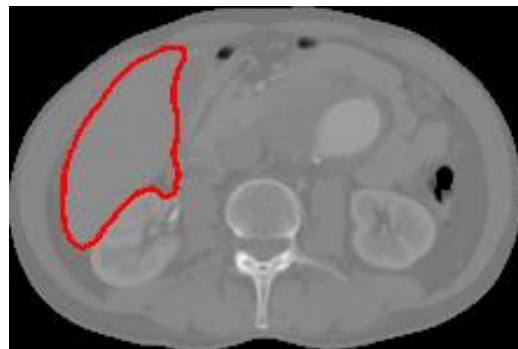


Figure 6: Segmentation at first level

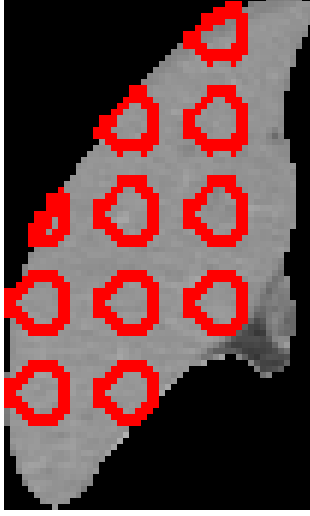


Figure 7: Initialization of second level segmentation

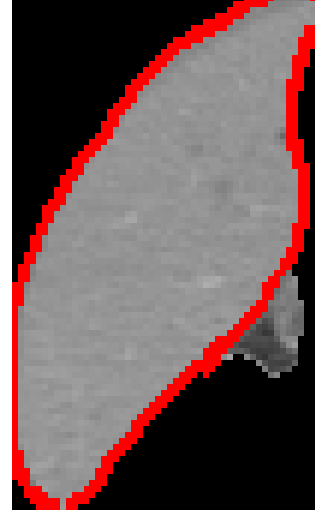


Figure 8: Segmentation at second level

The minimization process is stopped when the value of the functional is fluctuating about a certain value for a number of iterations. The output of this step is a BSP tree and a corresponding set of geometric wavelets. In the final step the Active Geometric Wavelets are ordered by their norm as in (1.4) and an approximation is created from the low resolution component and the largest n terms.

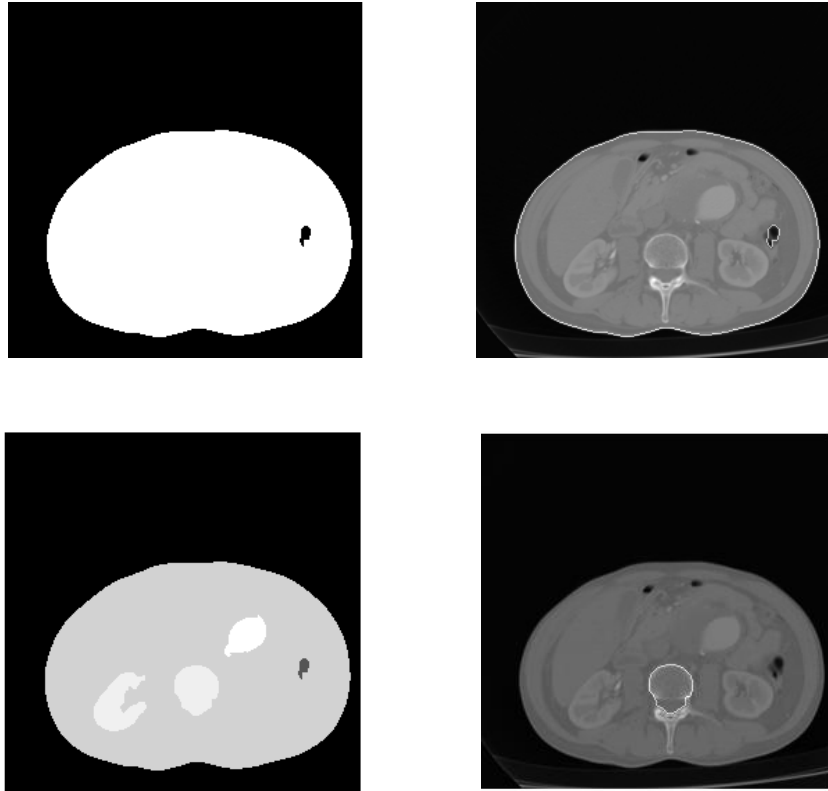
To summarize, this is the AGW algorithm:

-
1. *Creation of initial pixel groups:*
 - a. (Optional) Create a pre-processed input image for this step by applying anisotropic diffusion to the original image.
 - b. For each pixel p in the picture
 - i. If not part of a pixel group, create a new candidate pixel group and add p to the group,
 - ii. For every unprocessed pixel q in group: if one of its 4-connected neighbors r does not belong to another group and $|I(r) - I(q)| < \varepsilon$ (for some threshold ε), add r to the group.
 - c. Sort groups according to size and discard groups whose size is smaller than a threshold.
 2. Initialize a BSP tree with the root $\left\{ \left(I, \mathcal{Q}_{[0,1]^2} \right), \psi_{[0,1]^2} \right\}$.
 3. For every leaf $\{\Omega, \psi_\Omega\}$ in the tree, if the approximation error is larger than a threshold
 - a. Create an initialization curve. If the domain Ω contains pixel groups from step 1, then the initialization curve is determined from the largest such contained group. Else the initialization is a grid of small circles intersected with Ω .
 - b. Minimize the local Active Contour functional with large μ .
 - c. Repeat previous step, diminishing μ until a valid non-empty segmentation is found.

- d. Create and add to BSP two leaves corresponding to the two sub-regions found in step 3.c.
 4. Sort the Active Geometric Wavelets according to (1.4): $\psi_{\Omega_1}, \psi_{\Omega_2}, \dots$
 5. For a given n , the output of the algorithm is the n -term approximation $\psi_{[0,1]^2} + \sum_{i=1}^n \psi_{\Omega_i}$.
-

4 Experimental Results

Below, in Figure 9 we show an example of medical image segmentation which is one of the potential applications of our AGW method. On the left we see the segmentation that is derived from the n -term Active Geometric Wavelet approximation with n increasing (for several values of n). We see that with more terms added, the algorithm correctly adds the various organs of the body. On the right, we show the compact support of the wavelet that is added at that particular step, i.e. the n -th term.



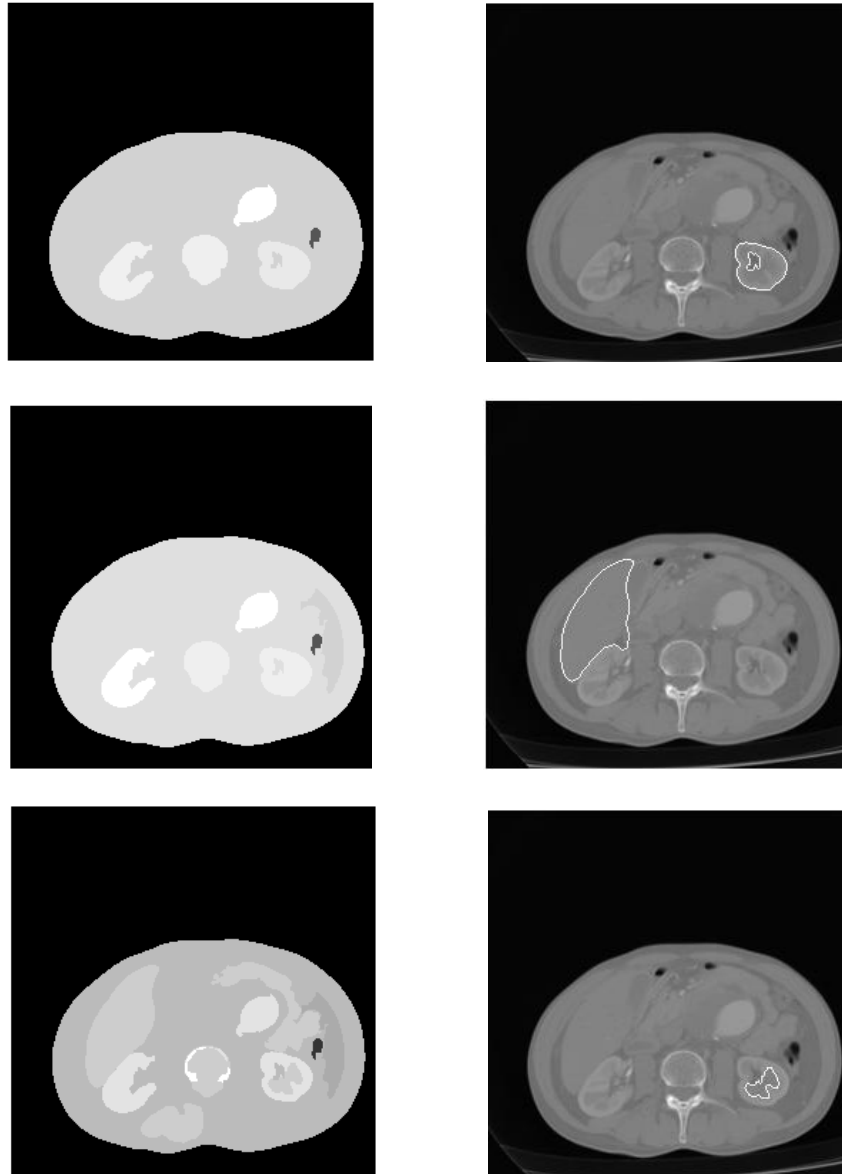


Figure 9 Adding Active Geometric Wavelet terms to the approximation

References

1. S. Brenner and L. Scott, The mathematical theory of finite elements methods, Springer-Verlag, 1994.
2. T. Chan and L. Vese. Active contours without edges. IEEE Trans. Image Processing, vol. 10, no.2, 266-277, February 2001.
3. G. Chung and L. Vese , Image segmentation using a multilayer level-set approach, Computing and Visualization in Science 12 (2009), 267-285.
4. A. Cohen, Numerical analysis of wavelet methods, Elsevier Science, 2003.

5. S. Dekel and D. Leviatan, Adaptive multivariate approximation using binary space partitions and geometric wavelets, *SIAM Journal of Numerical Analysis*, 43 (2005), 707-732.
6. R. DeVore, Nonlinear approximation, *Acta Numerica* 7 (1998), 51-150.
7. F. John, Extremum problems with inequalities as subsidiary conditions, *Studies and Essays Presented to R. Courant on his 60th Birthday*, Interscience Publishers, 1948, 187–204.
8. B. Karaivanov and P.Petrushev, Nonlinear piecewise polynomials approximation beyond Besov spaces, *Applied and Computational Harmonic Analysis* 15 (2003), 177-223.
9. R. Kazinnik, S. Dekel and N.Dyn, Low bit-rate image coding using adaptive geometric piecewise polynomial approximation, *IEEE Trans. Image Processing* 16 (2007), 2225-2233.
10. S. Lankton and A. Tannenbaum, Localizing Region-Based Active Contours, *IEEE Transactions on image processing* 17 (2008), 2029 – 2039.
11. S. Osher and R. Fedkiw, *Level Set Methods and Dynamic Implicit Surfaces*. New York: Cambridge Univ. Press, 2003.
12. P. Perona, J. Malik, Scale-space and edge detection using anisotropic diffusion, *IEEE Transactions on Pattern Analysis and Machine Intelligence*, 12(7): 629-639.
13. J.A. Sethian, *Level Set Methods and Fast Marching Methods*, 2nd edition, Cambridge University Press, 1999.